# Measurement

# Dual-luminescence Imaging and Particle Imaging Velocimetry for Simultaneous Temperature and Velocity Field Measurements in Immiscible Liquid --Manuscript Draft--

Manuscript Number:	
Article Type:	Research Paper
Keywords:	Luminescence technique; dual-luminescence imaging; particle imaging velocimetry; simultaneous temperature; velocity field measurement
Corresponding Author:	Hirotaka Sakaue, PhD University of Notre Dame Notre Dame, IN UNITED STATES
First Author:	Tatsunori Hayashi, PhD
Order of Authors:	Tatsunori Hayashi, PhD
	Hamed Farmahini Farahani, PhD
	Ali S Rangwala, PhD
	Hirotaka Sakaue, PhD
Abstract:	Arctic oil spills are particularly detrimental as they cause extensive ice melting in addition to the environmental pollution they create. However, few studies have been undertaken to reveal how oil-ice interactions impact ice melting. A simultaneous measurement method is developed to investigate the heat transfer pathways from oil slicks to ice. Functional luminescent probes are dissolved in a liquid immiscible with water, which imitates spilled oil. Another luminescent probe is added to seeding particles in order to increase their luminescent intensity. Dual-luminescence imaging and particle imaging velocimetry (PIV) are combined into a single simultaneous measurement method. The developed measurement system shows simultaneous temperature and velocity measurements for natural convection of the immiscible liquid. Successful implementation of the two measurement techniques together is a step toward analyzing heat transfer pathways in a spilled oil adjacent to an ice body, which indicates the extent of melting.



# College of Engineering

AEROSPACE AND MECHANICAL ENGINEERING

Journal

Measurement **Publication Type** 

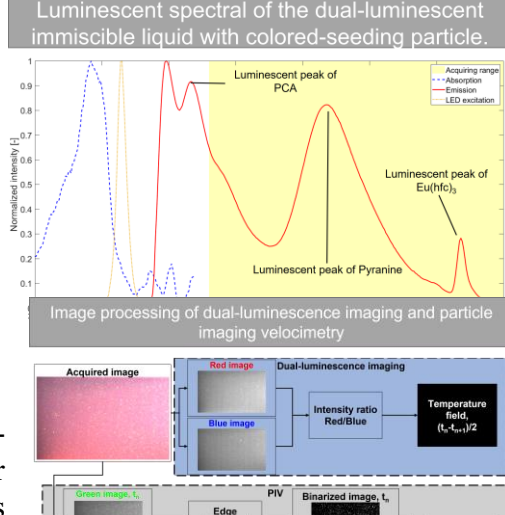
Research Paper

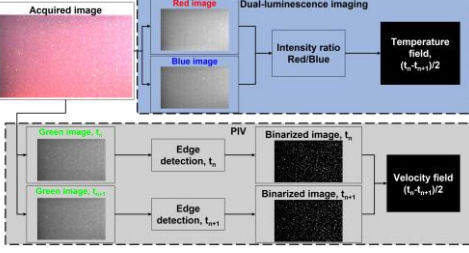
Title

Dual-luminescence Imaging and Particle Imaging Velocimetry for Simultaneous Temperature and Velocity Field Measurements in Immiscible Liquid

Dear Editor,

I am pleased to submit our original research article, "Dualluminescence Imaging and Particle Imaging Velocimetry for Simultaneous Temperature and Velocity Field Measurements in Immiscible Liquid," by Dr. Tatsunori Hayashi, Dr. Hamed Farmahini Farahani, Dr. Ali S. Rangwala, and Dr. Hirotaka Sakaue, for publication in *Measurement*. We developed the





simultaneous measurement method of thermometry and velocimetry for the immiscible liquid. The manuscript describes the components of the development of simultaneous measurements.

In this manuscript, we prepared the dual-luminescent solution with the colored-seeding particles, which gives three different luminescent intensities. The color camera captures those three intensities by three color channels simultaneously. The image processing provides the temperature distribution by the dual-luminescence imaging as well as the velocity field by the particle imaging velocimetry. As the demonstration of the developed measurement method, the temperature and velocity field of

the natural convection was captured.

This manuscript would give scientific contributions to Measurement and its readers. We would like to ask you to consider a review to be published in *Measurement*. This manuscript has not been published and is not under consideration for publication elsewhere. Both authors have approved the manuscript and agree with its submission to Measurement.

Thank you for your consideration, Tatsunori Hayashi

Tatsunori Hayashi, Ph.D.

Postdoctoral Research Associate, University of Notre Dame thayashi@nd.edu

Temperature distribution and velocity vectors of the side cooled cavity at steady-state 0.9 0.8 0.7 ₹ 0.5 0.2

Highlights (for review)

# Highlights

- Dual-luminescence imaging and PIV were integrated for simultaneous measurement.
- Pyranine added luminescent intensity to particles to separate other luminescence.
- Temperature and velocity of natural convection were captured as a demonstration.
- Simultaneous measurement provided the spatiotemporal temperature and velocity.
- Dual luminescent probes provide spatiotemporal temperature information of flow.

Declaration of Interest Statement

**Declaration of interests** 

oximes The authors declare that they have no known competing financial interests or personal relationships that could have appeared to influence the work reported in this paper.			
☑The authors declare the following financial interests/personal relationships which may be considered as potential competing interests:			
None			

#### Title:

Dual-luminescence Imaging and Particle Imaging Velocimetry for Simultaneous Temperature and Velocity Field Measurements in Immiscible Liquid

#### **Author names and affiliations:**

#### 1. Tatsunori Hayashi

Department of Aerospace and Mechanical Engineering, University of Notre Dame, Notre Dame, IN 46556, USA

E-mail: thayashi@nd.edu

#### 2. Hamed Farmahini Farahani

Department of Fire Protection Engineering, Worcester Polytechnic Institute, Worcester, MA, 01609, USA

E-mail: <u>hfaramahinifaraha@wpi.edu</u>

## 3. Ali S. Rangwala

Department of Fire Protection Engineering, Worcester Polytechnic Institute, Worcester, MA, 01609, USA

E-mail: <u>rangwala@wpi.edu</u>

#### 4. Hirotaka Sakaue

Department of Aerospace and Mechanical Engineering, University of Notre Dame, Notre Dame, IN 46556, USA

E-mail: <u>hsakaue@nd.edu</u>

#### **Corresponding author:**

Hirotaka Sakaue

E-mail: <u>hsakaue@nd.edu</u>

#### **Abstract**

Arctic oil spills are particularly detrimental as they cause extensive ice melting in addition to the environmental pollution they create. However, few studies have been undertaken to reveal how oil-ice interactions impact ice melting. A simultaneous measurement method is developed to investigate the heat transfer pathways from oil slicks to ice. Functional luminescent probes are dissolved in a liquid immiscible with water, which imitates spilled oil. Another luminescent probe is added to seeding particles in order to increase their luminescent intensity. Dual-luminescence imaging and particle imaging velocimetry (PIV) are combined into a single simultaneous measurement method. The developed measurement system shows simultaneous temperature and velocity measurement for natural convection of the immiscible liquid. Successful implementation of the two measurement techniques together is a step toward analyzing heat transfer pathways in a spilled oil adjacent to an ice body, which indicates the extent of melting.

\*Keywords: Luminescence technique, dual-luminescence imaging, particle imaging velocimetry,

# Nomenclature

 $V_R$  [V] Red image

simultaneous temperature, and velocity field measurement

 $V_B$  [V] Blue image

G	[-]	Geometric factor
$I_{Eu}$	[count]	Temperature-dependent luminescent intensity
$I_{PC}$	[count]	Temperature independent luminescent intensity
N	[count]	Noise of camera image
T	[°C]	Temperature measured by the dual-luminescence imaging
R	[-]	Ratio of luminescent images between the temperature-dependent/independent
A	[-]	Constant by second polynomial fitting for dual-luminescence imaging
В	[1/°C]	Constant by second polynomial fitting for dual-luminescence imaging
С	[1/°C²]]	Constant by second polynomial fitting for dual-luminescence imaging
Cr	[-]	Cross-correlation between the luminance-intensities
σ	[%]	Temperature sensitivity of dual-luminescence imaging
V	[mm/sec]	Velocity vector
$V_m$	[mm/sec]	Velocity magnitude
S	[mm]	Seeding particle displacement
t	[sec]	Measurement time
<i>x</i> , <i>y</i>	[-]	Location of measurement coordinate
α	[-]	Conversion factor between the imaging plane and the visualized physical plane

# **Subscripts**

 $[-]_{ij}$  Pixel location of camera images

 $[-]_{x,y}$  Direction of measurement coordinate

#### 1. Introduction

Tons of oil or chemicals are accidentally released into the environment each year [1]. Accidents around coastal areas harm the environment and have a negative impact on nature. Arctic oil spills are particularly detrimental as they can cause extensive ice melting in addition to the environmental pollution they create [2,3]. Floating oil slicks surrounding ice floes absorb energy from sunlight. However, only a few studies have been undertaken to reveal how oil-ice interactions impact ice melting [4–6]. In particular, melting caused by an adjacent immiscible liquid layer and heat transfer to ice is not well understood. Therefore, simultaneous temperature and velocity measurements in flow fields are required to understand the heat transfer mechanisms for an immiscible liquid layer.

Several works in the literature introduce methods to simultaneously measure both temperature and velocity to investigate heat transfer mechanisms in fluids [7]. The existing methods obtain the temperature in the fluid using dissolved functional chemicals. These methods generally measure velocity in the fluid by tracking dispersed particles in the liquid solution. For instance, Laser-Induced Fluorescence (LIF) relies on dispersed water-soluble luminescent probes in the liquid, which provide

temperature-sensitive fluorescence, to measure the temperature of an aqueous solution [8]. The LIF and particle-based velocimetry combination provides both temperature and velocity fields [9–11]. The experimental setup for simultaneous LIF and Particle Imaging Velocimetry (PIV) is generally complex, requiring extensive test equipment. Because images must be captured using multiple cameras for LIF and PIV, optical alignment and image registration require substantial post-processing [12]. Additionally, while the primary measurement target of LIF is aqueous solutions, research dealing with the temperature measurement for solvents such as oils and organic solvents is limited [7]. Molecular Tagging Velocimetry (MTV) and Thermometry (MTT) also capture the temperature and velocity field of a liquid simultaneously [13,14]. Thermochromic Liquid Crystal (LC) coupled up with PIV converts the color change of the LC to temperature [15]. These existing simultaneous measurement methods also use dissolved probes within a solvent. The use of dissolved probes allows for effective pixelbased measurements through the collection of fluorescent intensity or color change information from the liquid solution. While the high spatial resolution of these measurement methods is a large advantage, the type of the liquid solution and measurable temperature range is limited. In theory, these measurement methods function with all aqueous solvents, but organic solvents and oils pose challenges in terms of finding appropriate luminescent probes. Additionally, the measurable temperature range is narrow, as temperatures around zero degrees Celsius are not measurable. Particlebased thermometry is coupled with velocimetry utilizing functional particles for simultaneous

temperature and velocity measurement in fluids instead of the dissolved functional chemical in a solvent. Temperature Sensitive Particles (TSPs) are doped with luminescent probes that can be used to measure the temperature of fluids [7,16]. The seeding particles dispersed into the liquid solution give temperature-dependent luminescent intensity and can be used as tracers for particle-based velocimetry. The disadvantage of this particle-based temperature and velocity measurement is that the spatial resolution depends on the spacing between temperature-dependent luminescent particles. Areas between these particles must be interpolated, and so the average distance between these particles determines the spatial resolution of the temperature measurement.

In this research, a new simultaneous temperature and velocity field measurement method is developed by combining dual-luminescence imaging and PIV. The details of the developed measurement method are explained in sections 2 and 3. Dual-luminescence imaging gives spatiotemporal temperature information in both a liquid and a liquid-solid mixture [17]. The two luminescent probes used in dual-luminescence imaging have different fluorescent characteristics. One of the two luminescent probes emits a temperature-dependent luminescence. Another probe emits a temperature-independent luminescence. The luminescent peaks of the two probes lie at different wavelengths so that each luminescent peak can be acquired by a different color channel in a high-speed color camera. Each channel provides a different color image and by taking the ratio of the different color images, spatiotemporal temperature information of the liquid can be extracted [18].

One challenge in terms of applying a luminescent technique to study oil-ice interactions is the dynamic motion of ice as it is melting. As ice melts, its position changes, and with it the interface between the ice and the oil. Because of this dynamic motion, dual-luminescence imaging, which can capture temperature information over moving objects, is chosen as a unique diagnostic tool. PIV is a common technique for non-intrusive, quantitative, and qualitative flow visualization. In PIV, a thin sheet of light illuminates fluid containing reflective and neutrally buoyant seeding particles. The illuminated seeding particles allow for the visualization of the motion of a liquid. In this study, fluorescent PIV is combined with dual-luminescence imaging. The emission wavelength of the seeding particle must be separable from the fluorescence of the two luminescent probes in dual-luminescence imaging so that a separate channel of the high-speed camera can capture the luminescence from the colored seeding particles. If both dual-luminescent signals are separable from the seeding particle luminescence, a color camera can capture all luminescent emissions in separate red, green, and blue channels.

In this study, the immiscible liquid is prepared by dissolving two luminescent probes with distinct emission peaks. The luminescent seeding particles are then mixed with the prepared luminescent solution. A spectral measurement of the luminescent solution with the seeding particles is performed to confirm that the three emission peaks of the prepared solution match the sensor response of the color camera. The spectral measurement also allows for the determination of the temperature sensitivity of the luminescent solution. The behavior of flow with natural convection in a

side-cooled cavity is measured to demonstrate the developed simultaneous measurement method. The side-cooled cavity used here simply imitates a simplified version of the ice-oil interface without the melting process. The current results show that the convective field is directly coupled with the temperature field, i.e., the temperature difference instigates flow in the oil. Successful implementation of the two measurement techniques together is a step toward analyzing heat transfer pathways in a spilled oil adjacent to an ice body, providing insight into the melting extent.

#### 2. Background of luminescent imaging method

#### 2.1. Dual-Luminescence Imaging

The dual-luminescence imaging system is composed of an excitation light source, dual-luminescent liquid, and a color camera. The dual-luminescent immiscible liquid consists of temperature-dependent/independent luminescent probes. Under the excitation light, the dual-luminescent immiscible liquid absorbs energy. The dual-luminescent immiscible liquid subsequently emits light with two different peak wavelengths. The color camera captures the emitted fluorescence from the dual-luminescence immiscible liquid as luminescent intensities.

Consider the luminescent intensities from an arbitrary pixel, ij, on an image chip of the color camera, where the image chip has m by n pixels (i = 1, 2, ..., m, and j = 1, 2, ..., n). At this pixel, ij, the luminescent intensities from the blue image,  $V_{Bij}$ , and the red image,  $V_{Rij}$ , can be described as:

$$V_{Rij} = G_{ij} \cdot I_{Euij}(T) + N_{ij} \tag{1}$$

$$V_{Bij} = G_{ij} \cdot I_{PCij} + N_{ij} \tag{2}$$

where and  $I_{PC}$ are the luminescent intensities from europium [3- $I_{Eu}$ heptafluoropropylhydroxymethylene-camphorate] (Eu(hfc)<sub>3</sub>), and 1-pyrenecarboxylic acid (PCA), respectively. Because  $Eu(hfc)_3$  is a temperature-sensitive luminescent probe,  $I_{Eu}$ , has temperature dependency [19]. The functional notation (T), indicates the temperature sensitivity of the luminescent probe in equation 1. N indicates the camera shot noise at the pixel ij. The base shot noise can be obtained by collecting images without illumination. By taking an average of multiple noise images, the base shot noise can be obtained. Here, the geometric factor,  $G_{ij}$ , is a function of the pixel location. It is related to the shape and location of a liquid in an image frame, the nonuniformity of the illumination source, and the distance between the liquid and camera. Because the shape and location of a liquid can be changed during the measurement, the three factors above are time-dependent. To extract  $G_{ij}$  from the luminescent image, a luminescent ratio shown in equation 3 is taken.

$$R_{ij} = \left(V_{Rij} - \overline{N_{ij}}\right) / \left(V_{Bij} - \overline{N_{ij}}\right) = I_{Euij}(T) / I_{PCij}$$
(3)

Equation 3 allows for the canceling out of the geometric factor, giving a temperature-dependent intensity. As an image, R gives a temperature distribution. It can be obtained by taking the ratio of the red and blue images after subtracting the mean shot noise. At a pixel where  $I_{Euij}$  and  $I_{PCij}$  are near or equal to zero, the ratio of the two shown equation 3 would be undefined. To avoid this

processing error, a threshold can be assigned. For instance, if  $I_{Euij}$  or  $I_{PCij}$  are lower than the mean shot noise, the ratio, R, is assigned to be zero.

The intensity ratio exhibits a quadratic dependence on temperature. The relationship between the intensity ratio and temperature, *T*, can be expressed by a second-order polynomial [20]:

$$R = A + B \cdot T + C \cdot T^2 \tag{4}$$

where A, B, and C are coefficients of the second-order polynomial. These coefficients can be determined via experimental temperature calibration. The coefficient  $\sigma_T$ , or temperature sensitivity is defined as in equation 5:

$$\sigma_T = \frac{dR}{dT} = B + 2CT \,(\%) \tag{5}$$

In this research, the temperature sensitivity of the dual-luminescent immiscible liquid is calculated via *a priori* calibration based on the temperature measured by thermocouples.

#### 2.2. Particle image velocimetry

Particle image velocimetry (PIV) is a non-intrusive diagnostic tool that gives quantitative velocity information of a flow field. A thin light sheet illuminates seeding particles in the target fluid. The illuminated seeding particle allow for the visualization of the motion of the fluid, which can be either gaseous or liquid. A digital image sensor, which is positioned perpendicular to the sheet of light,

captures the motion of the particles. Two consecutive images of the illuminated plane are then captured with a time interval  $\Delta t$  between them. The displacement of particles between the consecutive images can be used to calculate velocities of the particles within the illuminated sheet over the time interval  $\Delta t$  [21]. The captured images are segmented into a number of small portions referred to as integration windows. The seeding particles in the integration window move to a new location within the time interval. This displacement is defined as  $\Delta s = (\Delta x, \Delta y)$ . Here,  $\Delta x$  and  $\Delta y$  are the displacement components with respect to the horizontal and vertical direction, respectively. The velocity vector, V, at a location (x, y) is derived by dividing the displacement,  $\Delta s$ , by time,  $\Delta t$ :

$$V(x,y) \approx \alpha \frac{\Delta s}{\Delta t} \tag{6}$$

where  $\alpha$  is the conversion factor between the imaging plane and the visualized physical plane. In a PIV method, the particle displacement,  $\Delta s$ , for groups of particles allows for the evaluation of the image via cross-correlation of many small sub-images based on the interrogation windows. This correlation evaluation yields the most probable displacement for a group of particles. The cross-correlation, Cr, between the luminance-intensity distribution,  $I_1(x, y)$ , at time t, and the luminance-intensity distribution,  $I_2(x, y)$ , at time  $t + \Delta t$  is calculated based on the luminescence-intensity distribution of the consecutive images by the equation:

$$Cr(\Delta x, \Delta y) = \iint I_1(x, y)I_2(x + \Delta x, y + \Delta y)dxdy \tag{7}$$

The cross-correlation forms a distribution and has a peak determining the average of the displacement

of the particles,  $\Delta s$ , within a window. Then, the velocity vector for the x and y direction can be calculated as follows:

$$V_x(x,y) = \frac{\Delta x}{\Delta t} \tag{8}$$

$$V_{y}(x,y) = \frac{\Delta y}{\Delta t} \tag{9}$$

where  $V_x$  and  $V_y$  are the x and y components of the velocity vector, respectively. Finally, the whole velocity vector of all interrogation windows is computed to obtain the velocity field. The velocity magnitude over the flow field is calculated by the equation:

$$V_{m}(x,y) = \sqrt{V_{x}(x,y)^{2} + V_{y}(x,y)^{2}}$$
(10)

#### 3. Simultaneous Temperature and Velocity Field Measurement

# 3.1. Dual-Luminescent immiscible liquid

For the dual-luminescence imaging of a liquid adjacent to ice, the spilled oil must be immiscible to water and dissolve the luminescent probes. In this research, toluene was selected to satisfy both these requirements. The concentration of the toluene in this work was 1 mM. Toluene as this dual-luminescent immiscible liquid contained two dissolved luminescent probes and colored seeding particles. One of the two luminescent probes provided temperature-dependent luminescence. The intensity of the other luminescent probe was independent of temperature. The two luminescent probes had peak luminescent emissions that could be separated from each other in terms of wavelength

so that they could be detected by different channels in a color camera. The two luminescent probes used in the dual-luminescent immiscible liquid were Eu(hfc)<sub>3</sub> (Sigma-Aldrich Corp., St. Louis, MO, USA), and PCA (Sigma-Aldrich Corp., St. Louis, MO, USA). PCA was selected for the temperature-independent luminescent probe because this luminescent probe has less temperature-dependence than Eu(hfc)<sub>3</sub>. Hollow glass microspheres (Cospheric, Santa Barbara, CA, USA) were mixed into the dual-luminescent immiscible liquid as colored seeding particles. The mean diameter of the seeding particles varied from 5 to 20 µm. The density of the seeding particles was 0.67 g/cc. Pyranine (Alpha Aesar, Tewksbury, MA, USA) was used to color the particles to give particles luminescence. It was dissolved in dichloromethane. The seeding particles were soaked in the dichloromethane. Then the dichloromethane was evaporated to prepare the colored seeding particles.

A spectrometer with a thermal stage was used to perform a temperature calibration of the dual luminescent immiscible liquid. The thermal stage controlled the temperature of the dual-luminescent immiscible liquid with the colored seeding particles. Figure 1 shows the absorption and emission spectra of the dual-luminescent toluene. Luminescent peaks are seen at 410, 510, and 610 nm. The peak at 410nm came from PCA. The peak at 610nm was due to Eu(hfc)<sub>3</sub>. Those emission peaks can be acquired by the blue and red channels of the color camera. The emission from Pyranine is located at 510nm, between the peaks of the dual-luminescent toluene. During the temperature calibration, the temperature of the toluene changed from -10 to 20 °C. The spectrometer captured the emission from

the developed dual-luminescence immiscible liquid. The emission of Eu(hfc)<sub>3</sub> changed its luminescent intensity during the calibration due to its temperature dependency [19]. The luminescent intensity was calculated by integrating the spectral output over a 50nm window centered at the emission peaks. Figure 2 shows the temperature calibration plot of the dual-luminescence toluene. The luminescent intensities from the luminescent probes were found by integrating the signal over the wavelength range from 430 - 480 nm for  $I_{PC}$  and from 580 - 630 nm for  $I_{Eu}$ . The calculated temperature sensitivity of the dual-luminescence immiscible liquid using equation 5 was -6.1 [%] at T = 5 °C. Here, error bars on each calibration point are based on the standard deviation from the three measurements with a 95% confidence interval.

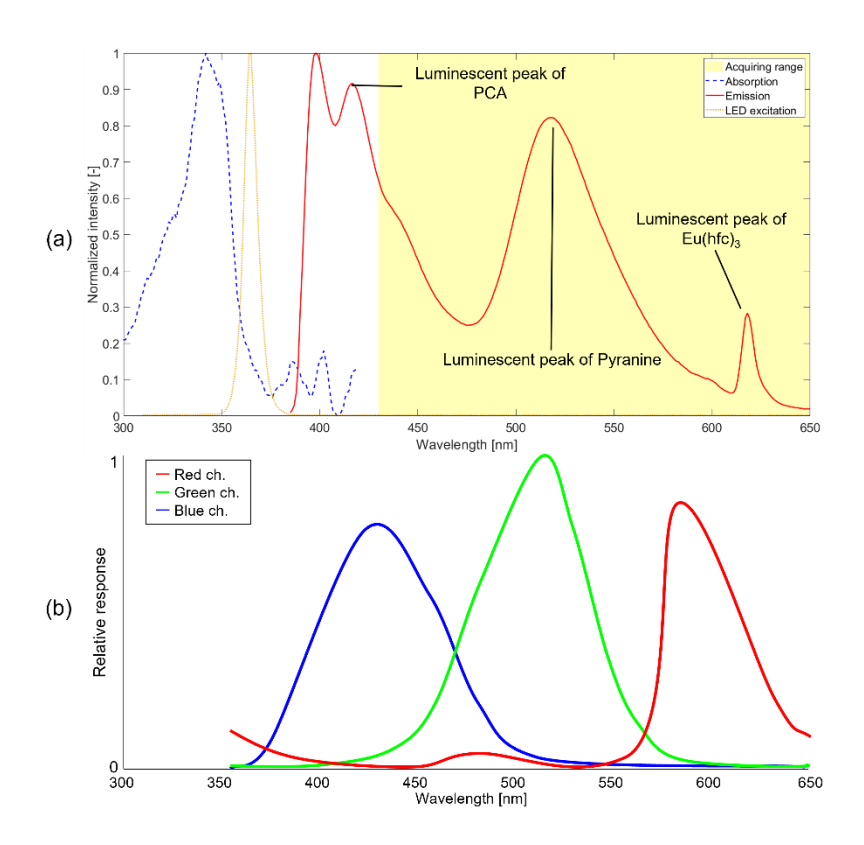


Figure 1 (a) Absorption and emission spectra of dual-luminescent immiscible liquid and (b) relative response of the color camera channels

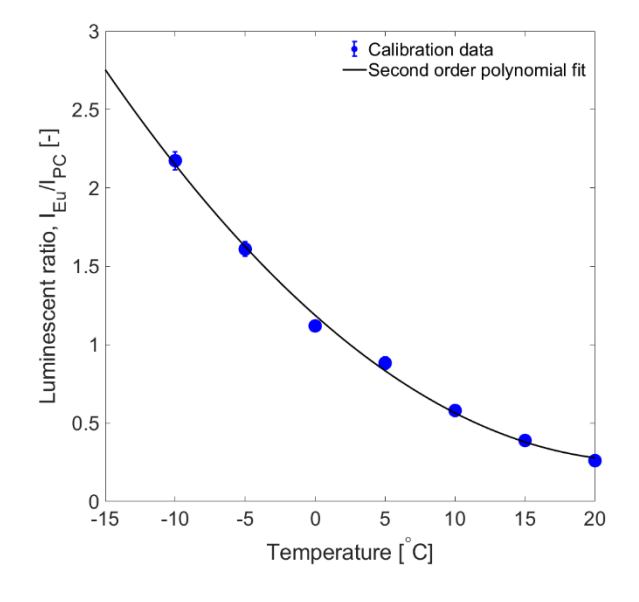


Figure 2 Temperature calibration plot of dual-luminescent immiscible liquid

#### 3.2. Measurement system

The flow regime selected for the demonstration of the simultaneous temperature and velocity field measurement was natural convection in a rectangle cavity. The measurement system is schematically described in Figure 3. The flow field was induced by a temperature difference between the Peltier cooler and the dual-luminescent toluene. The temperature difference was provided by cooling one side of the rectangle cavity. Natural convection occurred, which resulted in a 2-D velocity field and temperature distribution in the cavity. The measurement conditions imitate a simplified ice-oil interface in which the ice cools the adjacent oil but does not melt.

A rectangular quartz cuvette was used as the cavity and contained the dual-luminescent immiscible liquid with colored seeding particles. The inner dimensions of the cavity were  $40 \times 50 \times 10$  mm. The volume of the dual-luminescent immiscible liquid was 15 ml. The measurement system was placed in an environmental chamber that controlled the ambient temperature inside the chamber. The ambient temperature of the environment was set to  $18 \, ^{\circ}$ C. The Peltier cooler was set -20  $^{\circ}$ C to cool down one side of the cavity, with the remaining sides exposed to the ambient air.

The temperature distribution inside the cavity was obtained by the dual-luminescence imaging method (see section 2.1). The concentration of the two luminescent probes were 0.2 mM for Eu(hfc)<sub>3</sub> and 0.6 mM for PCA. The colored seeding particles had a concentration of 0.5  $\mu$ g/ml in the dual-luminescent immiscible liquid. Two 365nm UV-LED light sources excited the dual-luminescent

immiscible liquid and the seeding particles from the bottom and the side of the cavity. Excitation light was only allowed through 2mm slits on the bottom and side of the cavity. A high-speed color camera (MEMRECAM HX-7S, NAC Image Technology, Inc.) captured a time series of images during the simultaneous measurement. An optical long-pass filter was placed in front of the camera lens to cut off wavelengths shorter than 430 nm, which prevented the excitation light from entering the camera, as shown in Figure 3. The camera frame rate was 100 Hz and 40 total images were captured. The camera acquired images for two different purposes. The first was to track how the flow field changed with time. The second was to capture the flow field once it had reached steady state. To observe the change in the flow field, the camera acquired images for 200 seconds immediately after the Peltier cooler was placed on one side of the cavity. The detailed data processing procedure is explained in section 3.3. Before image acquisition for the steady flow field measurement began, thermocouple measurements confirmed that the temperature distribution had reached a steady-state. The thermocouple was removed from the liquid during image acquisition so as not to disturb the flow inside the cavity.

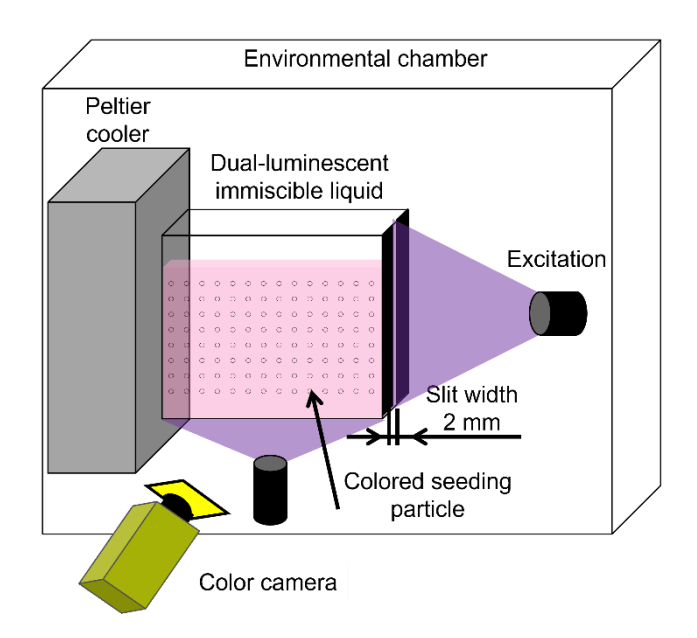


Figure 3 Schematic of dual-luminescence imaging and PIV measurement system.

## 3.3. Image processing

Figure 4 shows the image processing procedure for the dual-luminescence imaging and PIV.

The color camera captures the image with three different image sensors, red, green, and blue. The red and blue images are used for dual-luminescence imaging to measure the temperature distribution of the liquid. The green images track the motion of the seeding particles. These consecutive images are used for PIV analysis.

The red image contains the temperature-sensitive luminescent intensity from the Eu(hfc)<sub>3</sub> as well as the temperature- independent intensity such as reflected light. The blue image has only the temperature- independent intensity from PCA. The intensity ratio, the red image divided by the blue image, allows for extraction of the temperature-sensitive luminescent intensity. The luminescent

intensity ratio is calibrated by using temperature data captured by thermocouples. An *a priori* temperature calibration of the dual-luminescent immiscible liquid was performed for the demonstration. One hundred images were time-averaged to minimize the camera noise for each calibration temperature point.

PIV analysis used two consecutive green images to obtain a single velocity field. The green sensor in the camera captured the glare of the Pyranine-colored seeding particles distributed over the liquid. Because of the wide excitation range of the green channel of the camera, the green images contained the luminescence from the dual-luminescent immiscible liquid. An edge detection algorithm separated the intensity of the seeding particles from that of the dual-luminescent liquid. Binarized images were then used to identify the location of the seeding particles for PIV analysis. This processing was applied using built-in code in MATLAB before performing the PIV analysis. In this work, a GUI-based open-source tool (PIVlab) for PIV analyses in MATLAB was utilized [22]. The tool takes advantage of several built-in MATLAB features and eases subsequent data processing by providing a close link to the popular MATLAB user interface.

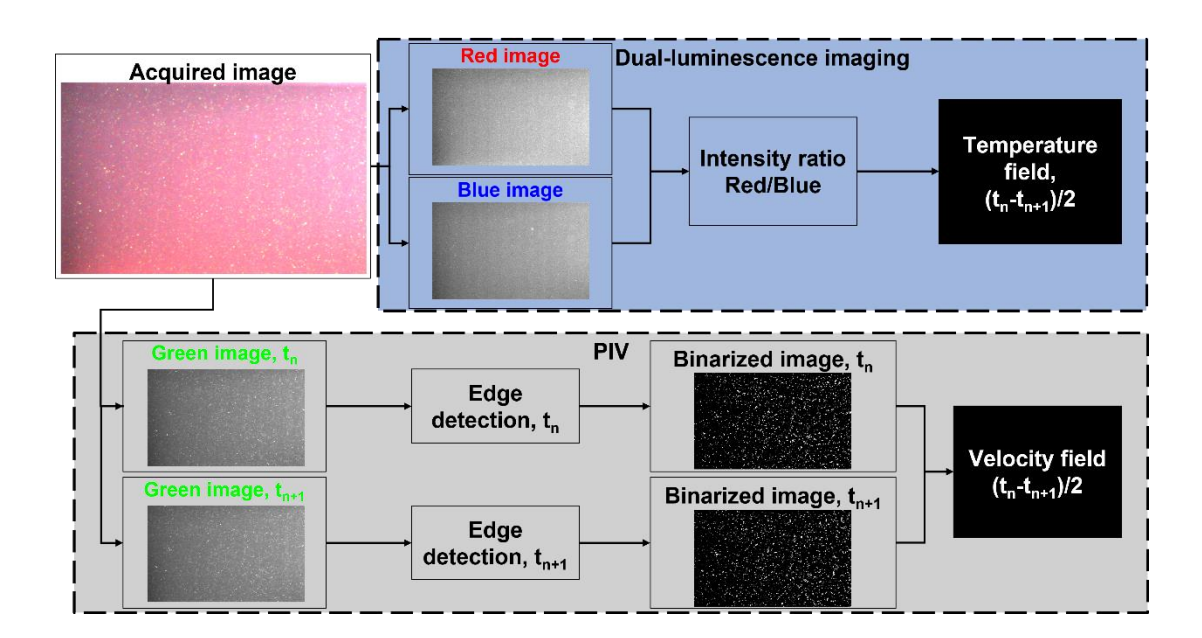


Figure 4 Image processing of dual-luminescence imaging and PIV.

### 4. Temperature and velocity field

# 4.1. Steady flow field

Figure 5 shows the temperature contour in the side cooled cavity at steady-state captured by dual-luminescence imaging as well as the superimposed velocity vectors calculated by PIV. The contour lines were drawn for 2.0°C intervals. The image acquisition started 30 min after cooling began. Thermocouples monitored the temperature in the cavity to ensure a steady-state had been reached. Thermocouples were removed from the cavity during the image acquisition. Because of overlap between the red, green, and blue channels of the color camera, pyranine luminescence leaked into the red and blue images. As a result, luminescent intensity near the seeding particles was removed from both the red and blue images. Image reconstruction using the least square method filled the gap left

by the removal of this luminescent intensity [23,24]. 40 consecutive red and blue images were timeaveraged to minimize the random noise of the camera before taking the intensity ratio. A spatial filter that averaged over 10 pixel x 10 pixel squares was applied to the raw intensity images. The image captured the 25 mm x 50 mm cavity with 880 pixels x 1530 pixels. The spatial resolution of the captured image was 32 mm/pixel in the x-direction and 28 mm/pixel in the y-direction. The top surface of the dual-luminescent liquid was open to the environment, and due to surface tension, exhibited some curvature. Due to this curvature and light reflection, the image around this free surface was blurred. Because of this, the image near the free surface was removed. This corresponded to approximately 1 mm in the vertical direction. This removal means the steep temperature gradient near the free surface was not observed. The left bottom corner of the quartz cuvette reflected the excitation light as well. Due to the high intensity of excitation light source present there, taking the ratio of the blue and red images could not completely cancel out the geometric factor of the illumination. Thus, there is a higher measurement uncertainty, which led to the apparently warmer temperature zone in the bottom left corner of the images. However, the overall temperature distribution on the cavity was successfully obtained. Lower temperature toluene is clearly visible along the cooled side. The temperature difference in turn induced a density gradient, which caused the colder toluene to sink to the bottom, which is what is seen in the temperature distributions. This is consistent with what is expected for buoyancy-driven flow inside a cavity. The colder temperature near the bottom of the

cavity was around -15 °C. The side of the cavity between the toluene and the Peltier cooler worked as an insulator. Because of this insulation, there is a slight temperature difference between the Peltier cooler and the toluene near the cooled side of the cavity. The other three sides of the cavity warmed up other areas of the toluene, which caused it to rise to the surface. The warmer temperature near the top surface was around 15 °C. The slight temperature difference between the ambient temperature and the toluene near the free surface was caused by the cropped zone mentioned above.

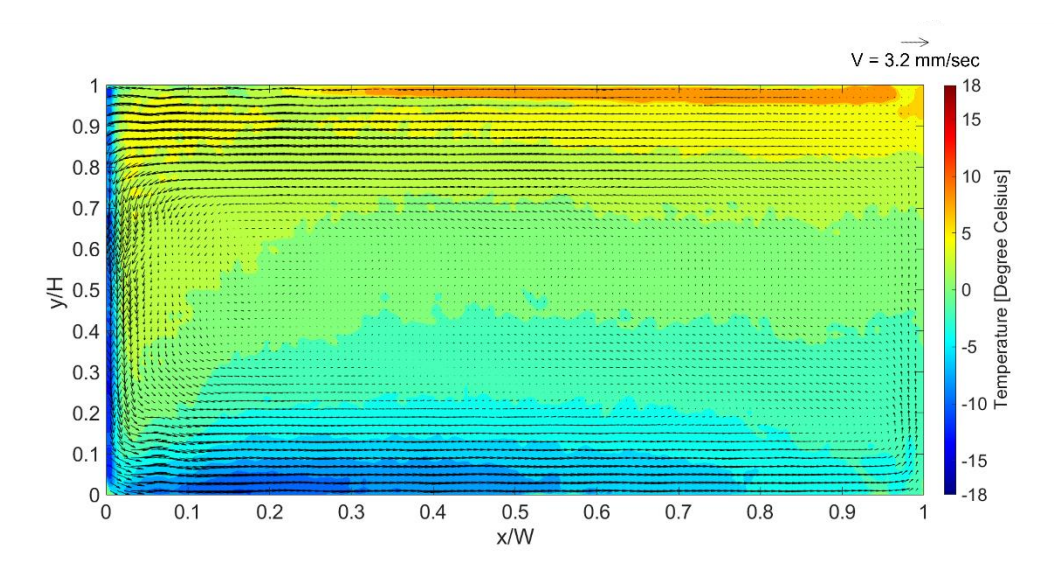


Figure 5 Temperature distribution of the side cooled cavity at steady-state captured by dualluminescence imaging and velocity vectors calculated using PIV.

Figure 6 shows the vector field and the velocity magnitude over the side cooled cavity calculated using PIV. The spatial resolution of the binarized image was the same as the initially captured image. The binarized images were calculated within each interrogation window of  $64 \times 64$  pixels with a 50% overlap for each ambient interrogation window. The spatial resolution of the PIV

analysis was 50 x 118elements. The spatial resolution for the velocity vector was 0.5 mm in the y-direction and 0.4 mm in the x-direction. This resolution was too coarse to resolve the velocity gradient within the velocity boundary layer on the cooled side. Higher velocity vectors can be seen near the cooled side of the cavity. This higher velocity field is due to the density gradient caused by the temperature variation. This temperature difference drove the circulation through the entire cavity. Qualitatively speaking, both the thermal boundary layer zone and the velocity boundary layer zone were observed near the cooled wall. The thermal boundary layer was thinner in the x-direction than the velocity boundary layer. This is expected for a boundary layer with a Prandtl number greater than 1. The Prandtl number of toluene is between 7 – 9 for the temperature range in the cavity.

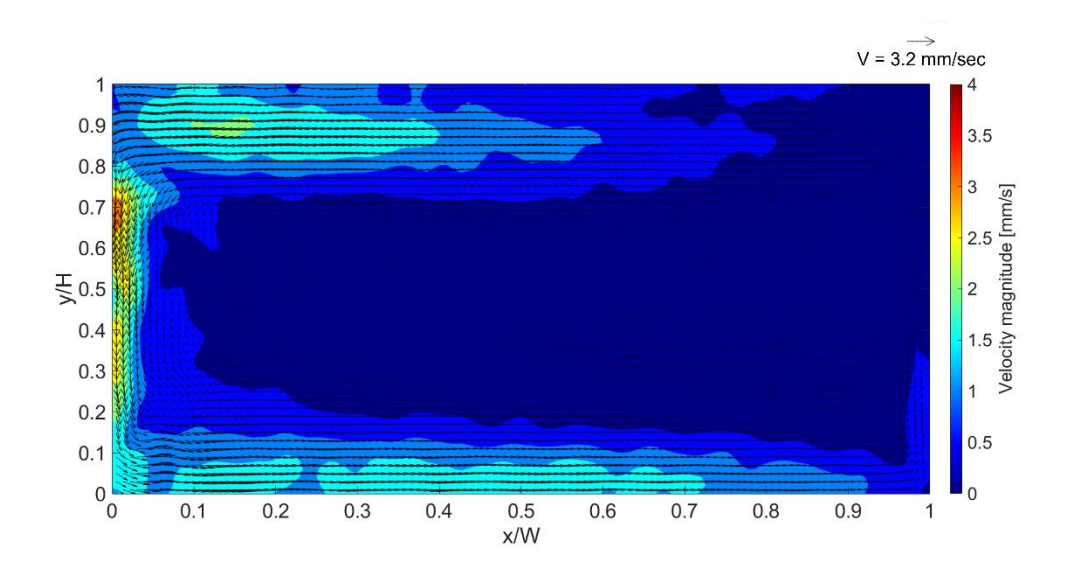


Figure 6 Velocity vectors and velocity magnitude field of the side cooled cavity at steady-state captured by PIV.

## 4.2. Flow field with the time evolution

Figures 7 – 9 show the development of the flow field with temperature contours and velocity vectors. The first temperature contour was from 10 sec after cooling began, and the following temperature contours indicate the flow field at 100 sec and 200 sec after cooling. The contour lines were drawn for 1.0°C intervals. The image processing for all figures was the same as for the steady-state flow field. A patchy temperature distribution was observed for all flow fields. This is due to low-intensity red images. Compared to the steady-state flow field, the temperature was higher, which corresponded to lower intensity from Eu(hfc)<sub>3</sub> and a lower signal in the red channel. This could theoretically be remedied by lowering the frame rate, but 100 Hz was the slowest possible frame rate for the high-speed camera used in this demonstration. This undesired result is a limitation of the experimental equipment rather than the experiment method.

Figures 10 – 12 show the development of the velocity of the flow field. The velocity fields were unaffected by the higher temperatures because of the temperature- independent nature of Pyranine. Compared to the steady-state, higher magnitude velocity vectors along the cooled side were observed, especially at the beginning of the cooling. Due to the more significant density gradient caused by the temperature difference between the toluene and the cooled side, the flow exhibited higher acceleration. The faster velocity flow created a thicker velocity boundary layer. The thickness of the velocity boundary layer got thinner over time.

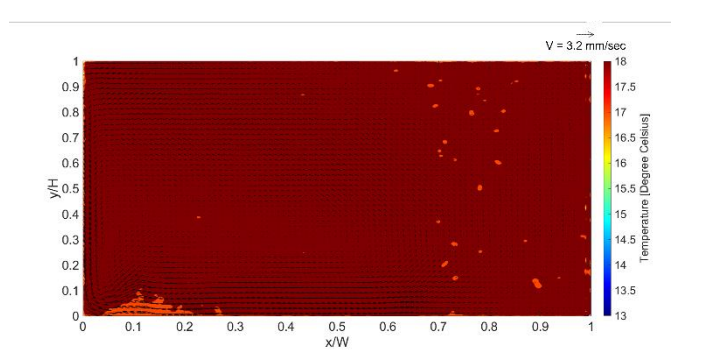


Figure 7 Development of the flow field with temperature contours and velocity vectors 10 sec after the cooling.

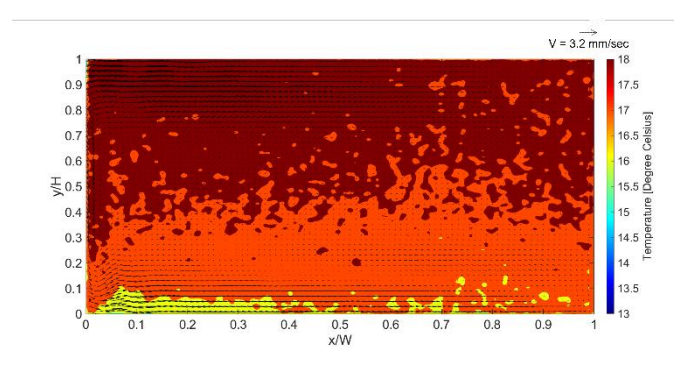


Figure 8 Development of the flow field with temperature contours and velocity vectors 100 sec after the cooling.

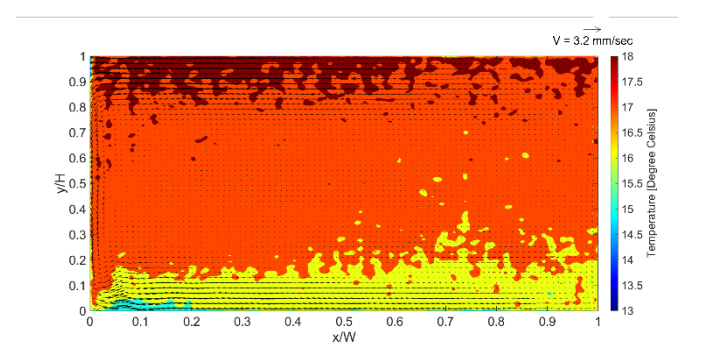


Figure 9 Development of the flow field with temperature contours and velocity vectors 200 sec after the cooling.

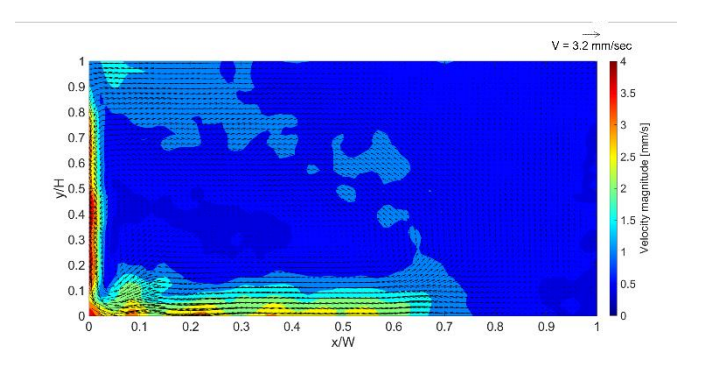


Figure 10 Development of the flow field with velocity magnitude contours and velocity vectors

10 sec after the cooling.

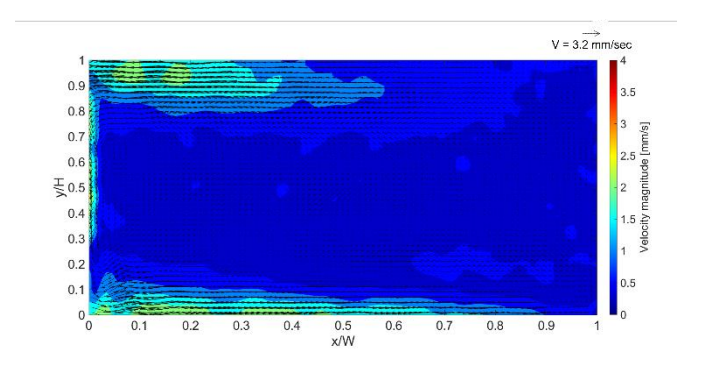


Figure 11 Development of the flow field with velocity magnitude contours and velocity vectors

100 sec after the cooling.

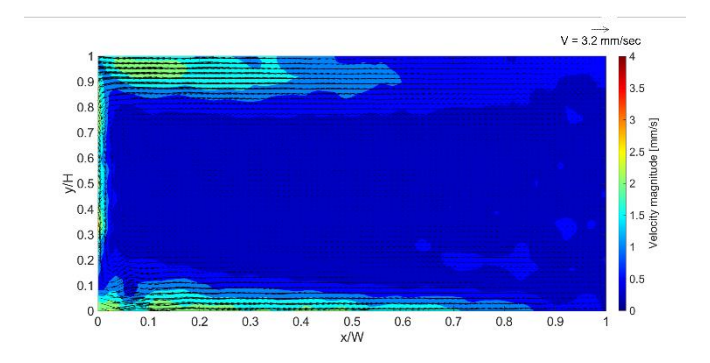


Figure 12 Development of the flow field with velocity magnitude contours and velocity vectors

200 sec after the cooling.

#### 5. Conclusion

A new simultaneous temperature and velocity measurement technique was developed by combining dual-luminescence imaging and particle-based velocimetry. For the dual-luminescence imaging, a dual-luminescent solution was developed. Toluene was selected as the immiscible liquid that imitates spilled oil over sea ice. Two luminescent probes were dissolved in toluene for dualluminescence imaging. One of the two luminescent probes is temperature-sensitive, and another one is temperature-insensitive. Europium tris [3-heptafluoropropylhydroxymethylene-camphorate] (Eu(hfc)<sub>3</sub>) was used for the temperature-sensitive luminescent probe, and 1-pyrenecarboxylic acid (PCA) was used for the temperature-insensitive probe. Hollow glass beads were colored with Pyranine to provide the luminescent intensity for seeding particles. Spectroscopic measurement confirmed that the luminescent spectra of the dual-luminescent solution with seeding particles had three peaks which matched the sensor response of the color camera. Two luminescent intensities of the dual-luminescent solution were captured by separate channels of a high-speed color camera. The remaining channel of the color camera captured the luminescent intensity of Pyranine-colored seeding particles for particlebased velocimetry.

As a demonstration of the developed simultaneous measurement method, a single cooled cavity was selected to capture the temperature and velocity distributions over the flow field. The single side-cooled cavity exhibited flow due to natural convection. Both steady and unsteady flow

measurements of this natural convection were collected with the simultaneous measurement technique. The developed measurement system simultaneously extracted 2-D temperature and velocity field information for the side cooled cavity. The extracted information is useful for analyzing the heat transfer pathway for spilled oil adjacent to ice, resulting in accelerated melting of this ice. The side-cooled cavity imitates the ice-oil interface without dynamic motion due to ice melting. As the final goal of this measurement method, simultaneous temperature and velocity field measurements of an immiscible layer adjacent to ice while it is melting will be conducted.

# Acknowledgements

This material is based upon work supported by the National Science Foundation under Grant No. 1938976 and No. 1938980. Any opinions, findings and conclusions or recommendations expressed in this material are those of the authors and do not necessarily reflect those of the National Science Foundation.

#### References

- [1] D.S. Etkin, Analysis of oil spill trends in the united states and worldwide, 2005 Int. Oil Spill Conf. IOSC 2005. (2005) 293–302. https://doi.org/10.7901/2169-3358-2001-2-1291.
- [2] E. Arzaghi, R. Abbassi, V. Garaniya, J. Binns, F. Khan, An ecological risk assessment model for Arctic oil spills from a subsea pipeline, Mar. Pollut. Bull. 135 (2018) 1117–1127.

- https://doi.org/10.1016/j.marpolbul.2018.08.030.
- [3] T. Nordam, D.A.E. Dunnebier, C. Beegle-Krause, M. Reed, D. Slagstad, Impact of climate change and seasonal trends on the fate of Arctic oil spills, Ambio. 46 (2017) 442–452. https://doi.org/10.1007/s13280-017-0961-3.
- [4] H. Farmahini Farahani, G. Jomaas, A.S. Rangwala, Effects of convective motion in n-octane pool fires in an ice cavity, Combust. Flame. 162 (2015) 4643–4648. https://doi.org/10.1016/j.combustflame.2015.09.021.
- [5] H.F. Farahani, W.U.R. Alva, A.S. Rangwala, G. Jomaas, Convection-driven melting in an n-octane pool fire bounded by an ice wall, Combust. Flame. 179 (2017) 219–227. https://doi.org/10.1016/j.combustflame.2017.02.006.
- [6] H. Farmahini Farahani, Y. Fu, G. Jomaas, A.S. Rangwala, Convection-driven cavity formation in ice adjacent to externally heated flammable and non-flammable liquids, Cold Reg. Sci. Technol. 154 (2018) 54–62. https://doi.org/10.1016/j.coldregions.2018.06.010.
- [7] S. Someya, Particle-based temperature measurement coupled with velocity measurement, Meas.
  Sci. Technol. 32 (2021). https://doi.org/10.1088/1361-6501/abc0b0.
- [8] J. Coppeta, C. Rogers, Dual emission laser induced fluorescence for direct planar scalar behavior measurements, Exp. Fluids. 25 (1998) 1–15. https://doi.org/10.1007/s003480050202.
- [9] R. Ibarra, O.K. Matar, C.N. Markides, Experimental investigations of upward-inclined stratified

- oil-water flows using simultaneous two-line planar laser-induced fluorescence and particle velocimetry, Int. J. Multiph. Flow. 135 (2021) 103502. https://doi.org/10.1016/j.ijmultiphaseflow.2020.103502.
- [10] B. Peterson, E. Baum, B. Böhm, V. Sick, A. Dreizler, Evaluation of toluene LIF thermometry detection strategies applied in an internal combustion engine, Appl. Phys. B Lasers Opt. 117 (2014) 151–175. https://doi.org/10.1007/s00340-014-5815-0.
- [11] S. Funatani, N. Fujisawa, H. Ikeda, Simultaneous measurement of temperature and velocity using two-colour LIF combined with PIV with a colour CCD camera and its application to the turbulent buoyant plume, Meas. Sci. Technol. 15 (2004) 983–990. https://doi.org/10.1088/0957-0233/15/5/030.
- [12] J. Sakakibara, R.J. Adrian, Whole field measurement of temperature in water using two-color laser induced fluorescence, Exp. Fluids. 26 (1999) 7–15. https://doi.org/10.1007/s003480050260.
- [13] F. Li, H. Zhang, B. Bai, A review of molecular tagging measurement technique, Meas. J. Int. Meas.

  Confed. 171 (2021) 108790. https://doi.org/10.1016/j.measurement.2020.108790.
- [14] H. Hu, Z. Jin, An icing physics study by using lifetime-based molecular tagging thermometry technique, Int. J. Multiph. Flow. 36 (2010) 672–681. https://doi.org/10.1016/j.ijmultiphaseflow.2010.04.001.
- [15] S. Funatani, N. Fujisawa, Simultaneous measurement of temperature and three velocity

- components in planar cross section by liquid-crystal thermometry combined with stereoscopic particle image velocimetry, Meas. Sci. Technol. 13 (2002) 1197–1205. https://doi.org/10.1088/0957-0233/13/8/306.
- [16] S. Someya, Y. Li, K. Ishii, K. Okamoto, Combined two-dimensional velocity and temperature measurements of natural convection using a high-speed camera and temperature-sensitive particles, Exp. Fluids. 50 (2011) 65–73. https://doi.org/10.1007/s00348-010-0894-0.
- [17] M. Tanaka, S. Kimura, K. Morita, H. Sakaue, Development and application of dual-luminescence imaging for capturing supercooled-water droplet under icing conditions, 5th AIAA Atmos. Sp. Environ. Conf. (2013) 1–7. https://doi.org/10.2514/6.2013-2548.
- [18] M. Tanaka, S. Kimura, K. Morita, H. Sakaue, Time-resolved temperature distribution of icing process of supercooled water in microscopic scale, Trans. Japanese Soc. Med. Biol. Eng. 51 (2013) 1–9. https://doi.org/10.2514/6.2014-2329.
- [19] Y. Egami, U. Fey, C. Klein, J. Quest, V. Ondrus, U. Beifuss, Development of new two-component temperature-sensitive paint (TSP) for cryogenic testing, Meas. Sci. Technol. 23 (2012). https://doi.org/10.1088/0957-0233/23/11/115301.
- [20] T. Hayashi, H. Sakaue, Temperature effects on polymer-ceramic pressure-sensitive paint as a luminescent pressure sensor, Aerospace. 7 (2020). https://doi.org/10.3390/AEROSPACE7060080.
- [21] M. Raffel, C.E. Willert, F. Scarano, C.J. Kähler, S.T. Wereley, J. Kompenhans, Particle Image

- Velocimetry, Springer, 2018. https://doi.org/10.3139/9783446436619.
- [22] W. Thielicke, E.J. Stamhuis, PIVlab Towards User-friendly, Affordable and Accurate Digital

  Particle Image Velocimetry in MATLAB, J. Open Res. Softw. 2 (2014).

  https://doi.org/10.5334/jors.bl.
- [23] K. Manohar, B.W. Brunton, J.N. Kutz, S.L. Brunton, Data-Driven Sparse Sensor Placement for Reconstruction: Demonstrating the Benefits of Exploiting Known Patterns, IEEE Control Syst. 38 (2018) 63–86. https://doi.org/10.1109/MCS.2018.2810460.
- [24] T. Inoue, Y. Matsuda, T. Ikami, T. Nonomura, Y. Egami, H. Nagai, Data-Driven Approach for Noise Reduction in Pressure-Sensitive Paint Data Based on Modal Expansion and Time-Series Data at Optimally Placed Points, Phys. Fluids. 077105 (2021) 077105. https://doi.org/10.1063/5.0049071.